Schweizerische Eidgenossenschaft
Confédération suisse
Confederazione Svizzera
Confederaziun svizra

Eidgenössisches Departement für
Umwelt, Verkehr, Energie und Kommunikation UVEK

Bundesamt für Energie BFE

APPLICATIONS OF MAGNETIC REFRIGERATION AND ITS ASSESSMENT

PROCEDURES FOR ANALYSES OF MAGNETIC REFRIGERATORS

Final report: Appendix 3

Performed by

Andrej Kitanovski, Marc Diebold, Didier Vuarnoz, Cyrill Gonin, Peter W. Egolf

Haute Ecole d'ingénerie et de Gestion du Canton de Vaud

Route de Cheseaux 1,

CH-1401 Yverdon les Bains

SWITZERLAND

peter.egolf@heig-vd.ch

www.heig-vd.ch

Impressum

Datum: *5. Juni 2008*

Im Auftrag des Bundesamt für Energie
Forschungsprogramm Elektrizitätstechnologien und -anwendungen

Mühlestrasse 4, CH-3063 Ittigen

Postadresse: CH-3003 Bern

Tel. +41 31 322 56 11, Fax +41 31 323 25 00

www.bfe.admin.ch

BFE-Bereichsleiter, thilo.krause@bfe.admin.ch

BFE-Vertrags- und Projektnummer: *101776 / 152191*

Bezugsort der Publikation: www.energieforschung.ch / www.electricity-research.ch

TABLE OF CONTENTS

1. MAXIMUM SPECIFIC COOLING ENERGY

The maximum specific cooling energy is directly related to the entropy and temperature change due to the magnetization/demagnetization of the magnetocaloric material. It is known that the maximum magnetocaloric effect of materials strongly depends on the temperature level (or e.g. Curie temperature). The highest magnetocaloric effect is obtained near or at the Curie temperature. However, the maximum cooling energy and the maximum temperature difference cannot be reached both in a single thermodynamic process (see Figure 1). The maximum specific cooling energy is obtained by an isothermal demagnetization at the Curie temperature (see Eq.1), while the maximum temperature change occurs by applying an adiabatic magnetization at Curie temperature.

$$q_{Cold(\max)} = T_C \ \Delta s(T_C). \qquad (1)$$

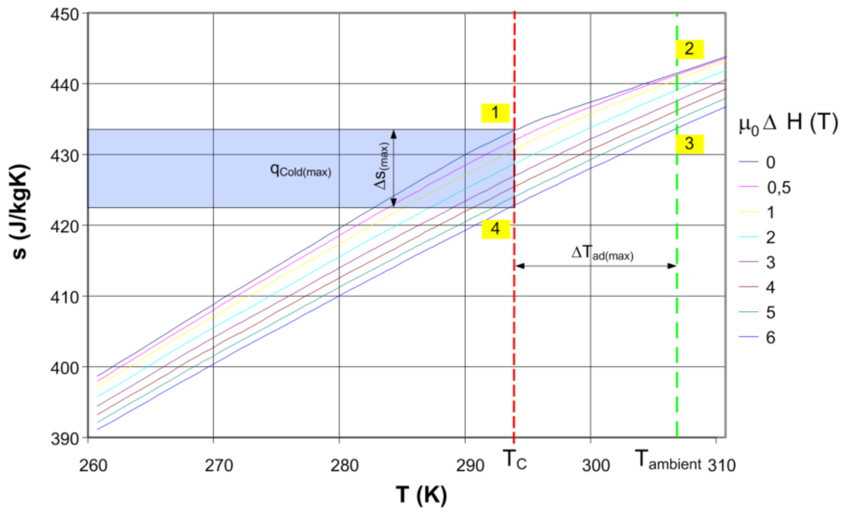

Figure 1: *The theoretical maximum specific cooling energy as a result of an isothermal demagnetization process in Gadolinium. The data for the diagram were taken from Ref. [1].*

One should note that the maximum specific cooling energy in Eq. (1) may be obtained in practice only within cycles, such as in the Ericsson cycle (two isomagnetic field processes, two isothermal processes) or the Stirling cycle (two isomagnetization processes, two isothermal processes), where a regenerative process is also applied. The Carnot cycle, which operates between two isotherms and two isentropes, cannot be performed with a so large specific cooling energy, when compared to the two before mentioned cycles. This is also shown in Figure 2.

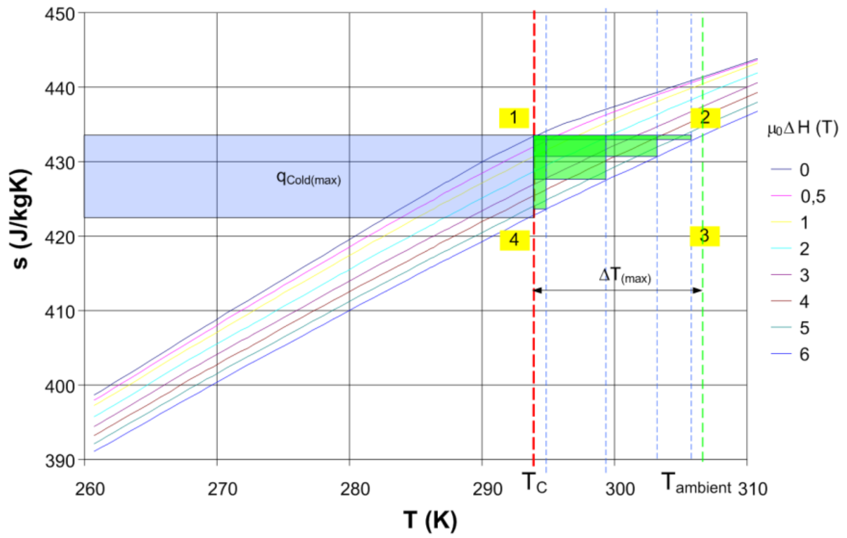

Figure 2: *Four different Carnot cycles in the s-T diagram: the ideal Carnot cycle gives the best efficiency, but does not present a high specific cooling energy and at the same time a high temperature span, what is usually required in practice. The maximum temperature span for the single stage Carnot cycle occurs in the limit of a specific cooling capacity being zero, and vice-versa the maximum specific cooling energy occurs in the limit of a temperature span equal to zero. The data for the diagram were taken from Ref. [1].*

Since the Ericsson or Stirling thermodynamic cycles require regeneration, they do not represent a simple, single stage cycle. A single stage cycle may be represented by e.g. the Brayton cycle, which operates between two isomagnetic fields and two isentropes and where no regeneration is performed. In practice, this would mean that the magnetocaloric sample is moved adiabatically from a certain initial temperature at a zero field to a certain magnetic field. In the higher isomagnetic field, heat is rejected from the magnetocaloric sample till the initial temperature of the magnetocaloric material is reached. Then the magnetocaloric material is moved out of the magnetic field, and therefore it cools adiabatically to a certain temperature below the initial one. In order to reach the initial temperature, heat has to be brought to the magnetocaloric sample and this heat represents the cooling energy. The maximum cooling energy in this type of cycle may be obtained, if the lowest temperature of the cycle is the Curie temperature. This temperature is reached by the isentropic demagnetization process (e.g. state 4 in the s-T diagram in Figure 3). The blue colored surface presents the maximum specific cooling energy for the Brayton cycle. Because state 4 is at the Curie temperature and the isentropic demagnetization started just at $T_C+\Delta T_{admax}$, we may define also other states for such basic cycles. The heat from the magnetocaloric material, in this specific example, may be rejected only until the initial temperature of the magnetocaloric material, before entering the magnetic field, is reached. Therefore, state 1 has the same temperature as state 3. From state 1, the adiabatic magnetization leads to an adiabatic temperature change, which is slightly lower than the maximum achievable at $\Delta T_{ad}(T_C+\Delta T_{ad}(T_C))$. Now state 2 is also defined. The maximum cooling energy for the single stage Brayton cycle may therefore be defined as:

$$q_R = \int_{s(T_C)}^{s(T_C+\Delta T_{ad}(T_C))} T\,ds = \int_{T_C}^{T_C+\Delta T_{ad}(T_C)} c_{H_0}\,dT . \qquad \text{(2a,b)}$$

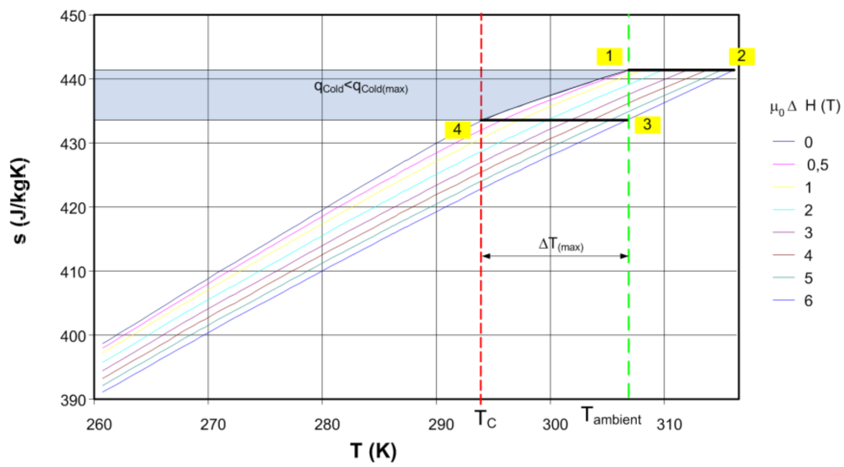

Figure 3: *The Brayton magnetic refrigeration cycle in a s-T diagram. The data for this diagram were taken from Ref. [1].*

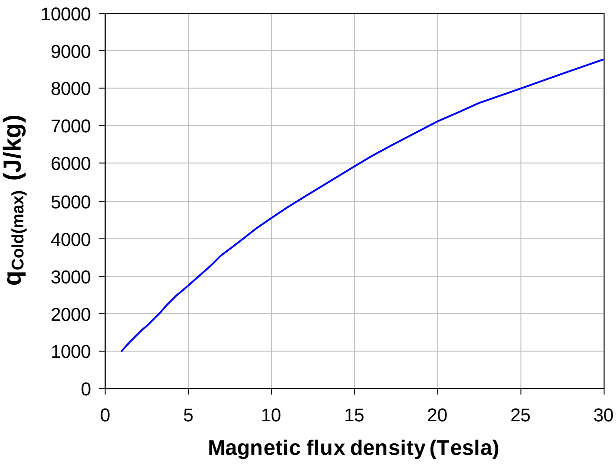

Figure 4: *Maximum theoretical specific cooling energy of Gadolinium depending on different magnetic flux densities. The data to produce this figure were taken from Ref. [1].*

For the purpose of the analysis, the data for the maximum specific cooling energy were defined for gadolinium, despite there exist many other types of magnetocaloric materials showing even higher values of specific cooling energy and adiabatic temperature difference. Figure 4 shows the data for the maximum specific cooling energy, based on the calculations, which were performed with Eq. (1).

2. GEOMETRY

In the analysis, the magnetocaloric material was considered to have the form of a coaxial ring, where a porous structure was realized by a tiny periodic structure. This kind of geometry was already described in the final report of the BFE project for heat pumps [2]. In this report slight modifications of the geometry were made in order to obtain a porous structure with a higher package degree (up to 30 volume percent) so that the power consumption required for the flow of the working fluid through it is not substantially or even not at all increased. The working fluid flows through a coaxial porous ring in axial direction.

2.1. THE CHARACTERISTICS OF THE CONCENTRIC MAGNETOCALORIC RINGS

The analysis shows that among different possible solutions of shapes of magnetocaloric material structures, a magnetocaloric ring, based on a periodic structure is in most cases the best possible solution. The fluid in such a ring may be applied axially or radially and in some cases (depending on the specifics of the structure) also in azimuth direction.

General characteristics

In order to have a good and fast heat transfer between the working fluid and the magnetocaloric material, the internal surface of the rotating magnetocaloric wheel must be very large. This may be realized in forms of packed beds of grains, foam like porous structures, in periodic structures such as parallel plates, honeycomb structures, wavy-like structures, etc. The internal flow diverters should prevent the working fluid to flow in undesired directions. Figure 5 shows two examples of the structure with packed beds of grains and with a periodic structure. The cross sectional area *A* of the wheel may be divided into the surface of the fluid with index *F* and the surface of the rotor (wheel) with index *R*.

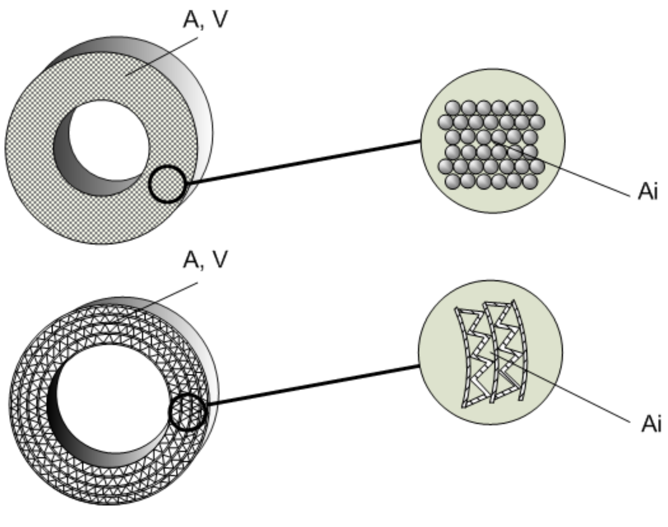

Figure 5: *A porous and a periodic structure with a cross sectional area A and a volume V.*

$$A = A_R + A_F \,. \tag{3}$$

Another characteristic area is the internal surface of the structure A_I, which should be very large in a magnetic cooling device. The following ratio can be defined:

$$\xi = \frac{A_I}{A_F} . \tag{4}$$

The packing fraction is a very important parameter:

$$\psi = \frac{V_R}{V} = \frac{V_R}{V_R + V_F} . \tag{5a,b}$$

Here V_R is the volume of the internal (magnetocaloric) material of the rotating wheel and V_F the volume of the wheel which is occupied by the working fluid.

The third important characteristic is the unit length:

$$\delta = \frac{V}{A_I} . \tag{6}$$

The wavy structure

The equations of the general characteristics are valid for all possible structures. Our knowledge and experience shows that a periodic structure like a wavy structure (which is well known in air-conditioning) will lead to several advantages when compared to the other kinds of structures:

- linear channels work also as flow diverters so they prevent a fluid flow in other undesired directions
- large internal surface
- small pressure losses compared to packed beds of grains
- simple manufacturing
- better resistance to mechanical stresses.

The geometric theory was already presented in Ref. [2]. Therefore only the final results which are important for the calculations are presented here. For a deeper study consult the mentioned reference.

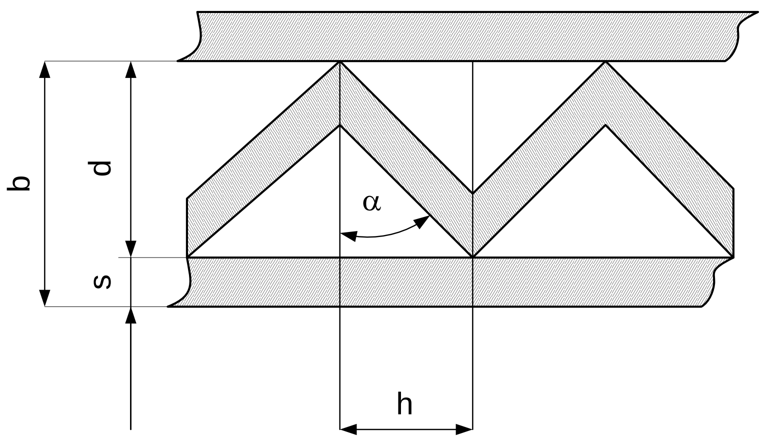

Figure 6: *The periodic porous structure can easily be produced. A triangle like folded sheet is put on the top of an even one and this is then winded up to give a heat exchanger as shown in Figure 5 in the lower part.*

Table 1: It shows the dimensions of the structure chosen for this analysis. The geometry was partly optimized in order to have the same pumping power losses even when the volume fraction of magnetocaloric material is increased, keeping the same mass flow of the working fluid. The consequence of this procedure is a thicker structure (*s* value increased), what influences the heat diffusion. However, it was already shown in a previous study [2] that the diffusion of heat into and out of the magnetocaloric material is fast for thicknesses of the sheets up to 0.5 mm.

Table 1: *Wave structures for magnetic refrigerators with different dimensions. The packing fraction varies from 10% to 30%. The values correspond to α=60°.*

Type	h (mm)	d (mm)	b (mm)	s (mm)	ψ (%)
1	3.359	2.055	2.155	0.1	10
2	3.568	2.336	2.575	0.239	20
3	3.814	2.708	3.146	0.438	30

With α=60 ° it follows that:

$$\chi = \frac{1}{\sin\alpha} = \frac{2}{\sqrt{3}} = 1.155. \tag{7a-c}$$

and:

$$\psi = \frac{(1+\chi)s}{d+s} \qquad \Leftrightarrow \qquad d = \left[\frac{(1+\chi)}{\psi} - 1\right]s. \tag{8a,b}$$

Further:

$$h = (d - \chi s)\tan\alpha = \sqrt{3}(d - \chi s). \tag{9a,b}$$

Another important geometrical parameter is defined as:

$$\xi = 2\frac{1+\chi}{d - \chi s}L, \tag{10}$$

where L is the length and:

$$\delta = \frac{1}{2}\frac{d+s}{1+\chi}. \tag{11}$$

3. THE PRESSURE LOSS IN THE PERIODIC STRUCTURE

Some of the most important losses which have a strong influence on the efficiency of the magnetic refrigerator are the irreversible losses due to the friction of the fluid. These losses are especially important in the magnetocaloric structure, where compactness with a large surface area to enhance the heat transfer is required. This leads some research groups to results with very low efficiency, influenced strongly by the pressure drop (see for example in Ref. [3]). The situation may be substantially improved by replacing the packed beds of grains by periodic structures and by applying a carefully selected design and operation characteristics.

The hydraulic diameter in the matrix of the periodic structure is defined as:

$$d_h = \frac{4A}{U}. \tag{12}$$

In Ref. [2] the hydraulic diameter is defined as:

$$d_h = 2\frac{d - \chi s}{1+\chi}. \tag{13}$$

Table 2: *The hydraulic diameter of the porous structure is defined with help of Eq. (13), which gives a basis for the calculation of the pressure losses in laminar flow.*

ψ	d_h (mm)
10	1.8
20	1.912
30	2.044

The Reynolds and Euler numbers are defined as:

$$\mathrm{Re} = \frac{v\, d_h}{\nu}, \qquad Eu = \frac{\Delta p}{\rho\, v^2}, \qquad \nu = \frac{\mu}{\rho}. \tag{14a-c}$$

Despite the pressure drop Δp gives a negative value, we will operate further with its absolute value. The friction coefficient is defined as:

$$\lambda = 2\frac{d_h}{L} Eu. \tag{15}$$

It follows for laminar flows:

$$\lambda = \frac{64}{\mathrm{Re}}. \tag{16}$$

With equations (15) and (16) one obtains:

$$\Delta p = \lambda \frac{L}{d_h} p_{dyn}, \qquad p_{dyn} = \frac{1}{2}\rho\, v^2. \tag{17a,b}$$

The specific pressure drop per unit of length is defined as:

$$R = -\frac{dp}{dx} = \frac{\Delta p}{L} = \frac{\lambda}{d_h} p_{dyn}. \tag{18a-c}$$

In household (or food) refrigerators rather harmless refrigerants and working fluids should be used. The proposed 25% methanol/water solution is a good working fluid, also for temperatures below the freezing point of water. One should note that a direct use of air or other gases as working fluid were not evaluated in this analysis. The goal of this study is to evaluate a liquid refrigerator, which may be used for any applications, including air conditioning.

The power which the pump requires to press the fluid through the periodic structure is:

$$P_{hyd} = \dot{V}\Delta p. \tag{19}$$

With Eq. (5a) one obtains:

$$1-\psi = 1-\frac{V_R}{V} = 1-\frac{A_R\, L}{A\, L} = 1-\frac{A_R}{A} = \frac{A-A_R}{A} = \frac{A_F}{A}. \tag{20a-e}$$

Because the pressure drop increases linearly with the length, the power loss per volume of the rotating wheel is a key quantity in the optimization process of a magnetic refrigerator:

$$\frac{P_{hyd}}{V} = \frac{\dot{V}\,\Delta p}{V} = \frac{\dot{V}}{A}\frac{\Delta p}{L} = (1-\psi)\frac{A_F\, v}{A_F} R = (1-\psi) v R. \tag{21a-d}$$

In the analysis, the velocity of the working fluid was defined in a dependence to the rotation frequency. A safety factor was taken into account in order to prevent a carry over leakage by the working fluid captured in the volume of the periodic structure at its boarders between hot and cold sides. Since the working fluid is operating between two main temperature levels of the heat source and the heat sink, the properties of the working fluid were taken at the average between the temperatures of the heat source and heat sink.

4. EQUATIONS FOR THE EFFICIENCY OF MAGNETIC REFRIGERATORS

The *COP* (Coefficient of Performance) of a refrigerator is a measure of the thermodynamic quality of such an apparatus. It shows how much electrical energy *W* has to be invested for a cooling or refrigeration task with a cooling energy Q_{cold}:

$$COP = \frac{Q_{cold}}{W} = \frac{\dot{Q}_{cold}}{P}. \qquad (22a,b)$$

In a process where the two energies are related to time continuous processes, taking the time derivatives of these two quantities does not change this ratio, and therefore Eq. (22b) is also correct. The cycle with the highest obtainable *COP* is the Carnot process. Its *COP* is expressed by the temperatures of the heat source T_{cold} and heat sink T_{hot}:

$$COP_{Carnot} = \frac{T_{cold}}{T_{hot} - T_{cold}} = \frac{\dot{Q}_{cold}}{P_{ideal}}. \qquad (23a,b)$$

The exergy efficiency compares a real or non-ideal cycle with this ideal cycle. Therefore, it is evident that the exergy efficiency of the Carnot cycle is one. The Carnot cycle is a reversible cycle.

The mechanical work to drive a magnetic refrigerator is usually coming from the turning of an electrical motor. Because this motor has some losses, one introduces a motor efficiency. In our analysis a characteristic value is assumed to be:

$$\eta_{Mot} = 0.9. \qquad (24)$$

Furthermore, a magnetic field leads to the driving of the magnetocaloric machine with some rectilinear or rotary movements of the magnetocaloric body. The magnetic field may induce some eddy currents, which lead to a further energy loss in the machine:

$$\eta_{Eddy} = 0.95. \qquad (25)$$

It is assumed that in porous structures these losses can be restricted to be only 5% of the total energy.

Another loss occurs if the magnetocaloric material shows a hysteresis:

$$\eta_{Hyst} = 0.97. \qquad (26)$$

It is well accepted that a magnetic cooler or refrigerator will usually have several cascade stages or regenerative steps. The number of stages depends on the temperature span between the heat source and the heat sink, the strength of the magnetic field, the heat transfer rate, etc. A heat transfer is always an irreversible process.

In Ref. [2] a method to determine the influence of such irreversibilities on the *COP* was presented. Here this method is further developed in such a manner that the heat transfer losses also result in a thermodynamic efficiency. In a cascade or regenerative process, as a matter of the heat transfer processes, different temperature differences occur. These are the following:

1) one at the source ΔT_{source}
2) one at the sink ΔT_{sink}
3) one between the material and the fluid on each side: $\Delta T_{stage, cold}$ and $\Delta T_{stage, hot}$.

In the previous report the entire temperature difference of one stage was denoted by ΔT_{loss}. To remind that this difference contains two heat transfer processes (the one on the cold and the one on the hot side) they are now each introduced by the quantities $\Delta T_{stage,\ cold}$ and $\Delta T_{stage,\ hot}$. In a first approximation we assume that these temperature differences are identical. This is indeed the case as a design will usually involve symmetric conditions and it can be assumed that in all stages the same fluid will be applied. Therefore, one may conclude that:

$$\Delta T_{stage} = \Delta T_{stage,cold} = \Delta T_{stage,hot} \,. \tag{S27a,b}$$

(S) denotes that this result is a special case. With this assumption it immediately follows that:

$$\Delta T_{loss} = \Delta T_{stage,cold} + \Delta T_{stage,hot} = 2\Delta T_{stage} \,. \tag{S28a,b}$$

It can be shown that the heat transfer losses can be taken into account by increasing the temperature difference:

$$\Delta T_{tot} = T_{hot} - T_{cold} \,. \tag{29}$$

In Eq. (24) one sees that qualitatively a higher value for this temperature difference occurring in the denominator decreases the *COP*. That is what one expects to occur! To now extend the temperature difference, it is defined to be:

$$\Delta T_{ext} = \Delta T_{tot} + \Delta T_{source} + \Delta T_{\mathrm{sink}} + n(\Delta T_{stage,cold} + \Delta T_{stage,hot}) \,. \tag{30}$$

Applying the approximation given in Eq. (S27a,b) and (S28b) to (30) one obtains:

$$\Delta T_{ext} = \Delta T_{tot} + \Delta T_{source} + \Delta T_{\mathrm{sink}} + 2n\Delta T_{stage} \,, \tag{S31}$$

respectively with Eq. (28a):

$$\Delta T_{ext} = \Delta T_{tot} + \Delta T_{source} + \Delta T_{\mathrm{sink}} + n\ \Delta T_{loss} \,. \tag{S32}$$

If in a further approximation one may assume that:

$$\Delta T_{source} = \Delta T_{\mathrm{sink}} \tag{S33a,b}$$

then one obtains from Eq. (S32):

$$\Delta T_{ext} = \Delta T_{tot} + 2\Delta T_{source} + n\ \Delta T_{loss} \,. \tag{S34}$$

This temperature difference is also the quantity which needs to be achieved by the adiabatic temperature changes of the magnetocaloric material in the different stages:

$$\Delta T_{ext} = n\ \Delta T_{ad} \,. \tag{35}$$

Now it follows immediately from Eq's (29) and (S34) that:

$$\Delta T_{tot} = T_{hot} - T_{cold} = \Delta T_{ext} - 2\Delta T_{source} - n\Delta T_{loss} \,. \tag{S36}$$

Substituting Eq. (35) into (S36) one obtains:

$$\Delta T_{tot} = n\ \Delta T_{ad} - 2\Delta T_{source} - n\ \Delta T_{loss} \,. \tag{S37}$$

When ΔT_{tot}, ΔT_{ad}, ΔT_{source}, ΔT_{loss} are known quantities, one is able to define the number of stages.

The *COP* of a multi-stage machine is now the one with the extended temperature difference:

$$COP_{Multi} = \frac{T_C}{\Delta T_{ext}} = \frac{T_C}{n\ \Delta T_{ad}} \ . \qquad (38a,b)$$

With Eq. (S37) for the *COP* of the Carnot process it follows:

$$COP_{Carnot} = \frac{T_C}{\Delta T_{tot}} = \frac{T_C}{n\ \Delta T_{ad} - 2\Delta T_{source} - n\ \Delta T_{loss}} = \frac{T_C}{n\ (\Delta T_{ad} - \Delta T_{loss}) - 2\Delta T_{source}} \ . \qquad (39a\text{-}c)$$

The efficiency for these heat transfer losses is given by:

$$\eta_{Multi} = \frac{COP_{Multi}}{COP_{Carnot}} \ . \qquad (40)$$

Substituting Eq. (38) and (39b) into (40) the result is:

$$\eta_{Multi} = \frac{n\ \Delta T_{ad} - 2\Delta T_{source} - n\ \Delta T_{loss}}{n\ \Delta T_{ad}} = 1 - \frac{\Delta T_{loss}}{\Delta T_{ad}} - \frac{2\Delta T_{source}}{n \Delta T_{ad}} \ . \qquad (S41a,b)$$

The following approximation is interesting and is valid when many stages occur:

$$\eta_{Multi} = 1 - \frac{\Delta T_{loss}}{\Delta T_{ad}}, \qquad n \gg 1. \qquad (S42)$$

In this special case one observes that the heat transfer efficiency does not depend on the number of stages. The reason is that for large temperature spans the COP_{Carnot} decreases and the losses are proportional to this quantity. If the loss ΔT_{loss} is equal to the adiabatic temperature change ΔT_{ad} the efficiency is zero.

Furthermore, a general heat gain in a refrigerator of 5% exergy loss is assumed to occur:

$$\eta_{Gen} = 0.95 \ . \qquad (43)$$

The last remaining loss is given by the pressure drop of laminar fluid flow through the porous structure. In Chapter 3 the theory to determine a «specific power loss» is outlined. Here specific means per volume unit.

We assume that the pressure loss is the same in all stages. Then if the loss by pressure drop of one stage is P_{hyd}, then for n stages this loss is:

$$P_{Hyd} = n\ P_{hyd} \ . \qquad (44)$$

Note that different sizes of initial letters are used to denote the «specific power loss» of a single stage P_{hyd} and of the total machine P_{Hyd}!

Now it follows that the pressure drop contribution relatively to the ideal Carnot *COP* is:

$$\eta_{Hyd}\ COP_{Carnot} = \eta_{Hyd}\ \frac{\dot{Q}_C}{P_{ideal}} = \frac{\dot{Q}_C}{P_{ideal} + P_{Hyd}} \ . \qquad (45)$$

Then one has:

$$\eta_{Hyd} = \frac{1}{COP_{Carnot}} \frac{\dot{Q}_C}{P_{ideal} + P_{Hyd}} \ , \qquad (46)$$

respectively:

$$\eta_{Hyd} = \frac{1}{1+\frac{P_{Hyd}}{P_{ideal}}}. \tag{47}$$

The final *COP* of a machine with several stages is:

$$COP_{Final} = \xi \, COP_{Carnot} , \tag{48}$$

with the exergy efficiency defined as:

$$\xi = \eta_{Mot} \, \eta_{Eddy} \, \eta_{Hyst} \, \eta_{Multi} \, \eta_{Gen} \, \eta_{Hyd} \cdot \tag{49}$$

The theory which has been presented is based on the assumption that the losses of heat transfer (*Multi*) and pressure drop of the flow (*Hydr*) occur in a quasi-homogeneous manner distributed over the entire temperature range of the refrigerator. If the different parts of a machine have different high losses, this theory will deviate slightly from reality. The first derivations for more complex situations with different sized stages are published in Ref. [4].

In the case of use of superconducting magnets, the efficiency of the refrigerator is further reduced due to the power demand for the magnetic field source and for the special kryo-cooling system. In the analysis it was assumed that this kind of losses in large scale devices reduce the efficiency by approximately 5%, thus leading to:

$$\xi = \eta_{Mot} \, \eta_{Eddy} \, \eta_{Hyst} \, \eta_{Multi} \, \eta_{Gen} \, \eta_{Hyd} \, \eta_{Sc} \cdot \tag{50}$$

where

$$\eta_{Sc} = 0.95. \tag{51}$$

Superconducting motors could be used in large scale systems. In this particular case this would influence the efficiency of the conversion of electrical power input into mechanical one. Therefore, it is assumed that η_{Mot}=0.95 instead of 0.90 (compare with Eq. (24)).

5. EVALUATION OF THE TOTAL MASS AND VOLUME

The cooling power of the device is required to determine the total mass and volume of magnetocaloric material. But one has to be aware that this mass of magnetocaloric material must be so large that its cooling capacity can also cover all the different losses. Therefore, also the operation conditions, the coefficient of performance and the number of stages are important to be known for such a determination. It is clear that this is actually an iterative process.

For an approximate determination the following equation may be applied:

$$m_{mc} = \frac{\dot{Q}_{tot}}{\nu \, q_{Cold(\max)}} \approx \frac{\left(\dot{Q}_C + \dot{Q}_H\right) n}{2 \nu \, q_{Cold(\max)}} = \frac{\left(2\dot{Q}_C + \frac{\dot{Q}_C}{COP}\right) n}{2 \nu \, q_{Cold(\max)}} . \tag{52a,b,c}$$

If the volume fraction ψ of the magnetocaloric porous structure is known, one is able to determine the total volume occupied by this structure:

$$V_{ps} = \frac{m_{mc}}{\rho_{mc} \, \psi} \tag{53}$$

Assuming that one half of the magnetocaloric ring is in the magnetic field and the other half outside, it follows that:

$$V_{gap} = \frac{m_{mc}}{2\rho_{mc}\,\psi} \tag{54}$$

By applying a finite element software a special numerical analysis was performed to determine the volume of the magnet assembly as a function of the magnetic field strength. The relation for large scale applications is the following:

$$V_{mag} = xV_{gap} = \left[(\mu_0\,\Delta H_0)^2 - \mu_0\,\Delta H_0 + 2\right]\,V_{gap}\,, \tag{55}$$

where the factor *x* is given by Figure 7. For small scale applications this relation is too optimistic and was replaced by the same formula, but multiplied by the factor three. Intermediate cases would show corresponding multipliers between 1 and 3, but such cases were not (yet) investigated.

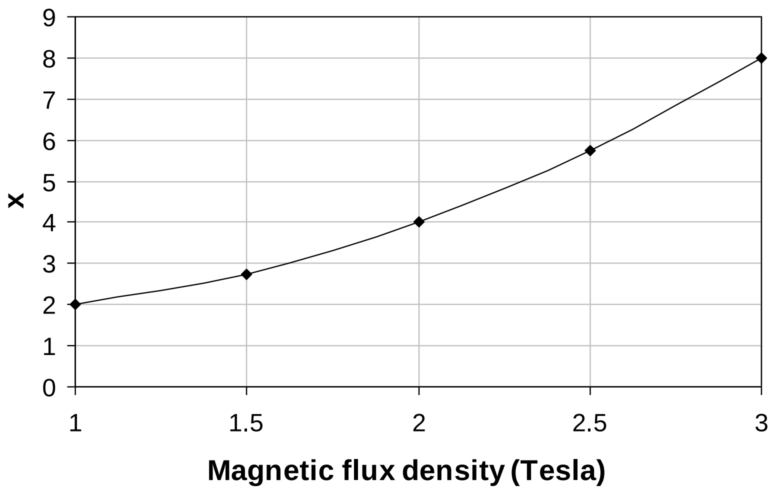

Figure 7: *The multiplication factor x for large scale refrigerating systems equipped with permanent magnet assemblies as a function of the magnetic field strength is shown. For intermediate and small machines the values are higher.*

The masses of the magnet assemblies were determined by taking a density of 7500 kg/m^3 for the magnet's material into consideration. The other components such as pipes, valves, motors, etc. also contribute to the total mass. However this contribution is relatively much higher for small scale machines than for larger ones. In order to simplify the evaluation of this mass, it was considered that taking approximately half of the total mass of a conventional compressor is an adequate recipe to calculate the mass of the ensemble of all these auxiliary elements.

The total volume of a magnetic cooler or refrigerator was defined as a three time larger volume than the one occupied by the volume of the permanent magnet assemblies including the volume occupied by the magnetocaloric porous ring. - It is absolutely clear that these considerations are rather rough approximations.

6. SYMBOLS

Standard

q	specific cooling energy (J/kg)
T	temperature (T)
s	specific entropy (J kg^{-1} K^{-1})
c	specific heat capacity (J kg^{-1} K^{-1})
H	magnetic field strength (A m^{-1})
A	surface (m^2)
V	volume (m^3)
U	perimeter (m)
d	diameter (m)
Re	Reynolds number
Eu	Euler number
R	specific pressure drop (Pa m^{-1})
p	pressure (Pa)
Q	cooling energy (J)
W	work (J)
$\dot{Q}$	heat flux (W)
n	number of stages
m	mass (kg)

Greek

μ	magnetic permeability (Wb, A^{-1} m^{-1})
ξ	surface ratio
ψ	packing factor
δ	characteristic length (m)
λ	friction coefficient
ρ	density (kg m^{-3})
η	efficiency
ξ	exergy efficiency

Indices

max	maximum
C	Curie, cold
ad	adiabatic
0	external, vacuum
I	internal
R	rotor
F	fluid
h	hydraulic
hyd	hydraulic
dyn	dynamic
Mot	motor
Eddy	eddy currents
Hyst	hysteresis
tot	total
ext	exterior
Multi	multi stage
Gen	general heat gain
Hyd	hydraulic for *n* stages
Sc	superconducting
ps	porous structure
mc	magnetocaloric
H	hot
mag	magnet

ACKNOWLEDGEMENTS

We thank the Swiss Federal Office of Energy (T. Kopp and R. Brüniger) and the Gebert Rüf Stiftung for financing our R&D activities.

REFERENCES

[1] R. E. Rosensweig, C. Gonin, A. Kitanovski, P.W. Egolf, Magneto-thermodynamics' charts of gadolinium for magnetic refrigeration (in preparation).

[2] P. W. Egolf, F. Gendre, A. Kitanovski, O. Sari, 2006, *Machbarkeitsstudie für magnetische Wärmepumpen: Anwendungen in der Schweiz.* Schlussbericht des Projektes zuhanden des Bundesamtes für Energie Nr. 100873/151017, 2006, pp. 1- 67.

[3] T. Okamura *et al.*, Improvement of 100 W class room temperature magnetic refrigerator, 2nd International Conference on Magnetic Refrigeration at Room Temperature, Portoroz, Slovenia, 2007, pp. 377-398.

[4] J. Varun, P. W. Egolf, *Application of magnetic refrigeration: A magnetic laboratory refrigerator.* Scientific report of a summer internship, Joint project of Indian Institute of Technology, Kampur, India, and University of Applied Sciences of Western Switzerland, Yverdon-les-Bains, Switzerland, 2007.